Med Chem Res (2012) 21:4290–4300
DOI 10.1007/s00044-011-9968-7

MEDICINAL CHEMISTRY RESEARCH

ORIGINAL RESEARCH

Two new halocuprates complexes [Cu^{II}(1,4,8,11-tetraazacyclotetradecane)][$Cu^{I}Cl_3$] and [H_4(1,4,8,11-tetrazacyclotetradecane)][$Cu^{I}_2Cl_6$]: synthesis, characterizations and biological studies

Mohammed Lachkar · Ilham Halime · Abdoulillah Bezgour · Brahim El Bali · Michal Dusek · Karla Fejfarova · Sadia Siddiq · Bishnu P. Marasini · Shagufta Noreen · Ajmal Khan · Saima Rasheed · M. Iqbal Choudhary

Received: 24 August 2011 / Accepted: 21 December 2011 / Published online: 13 January 2012
© Springer Science+Business Media, LLC 2012

Abstract Synthesis, crystal structures and biological activities for the new chlorobridged mixed valence Cu^{I}/Cu^{II} coordination polymer [Cu^{II}cyclam][$Cu^{I}Cl_3$] **1** and [H_4cyclam][$Cu^{I}_2Cl_6$] **2** are reported. Compound **1** crystallizes in the orthorhombic system, space group *Pccn*, with $a = 22.677(4)$, $b = 22.827(4)$, $c = 12.506(2)$ Å, $V = 6473.75(19)$ Å^3, $Z = 8$. Its crystal structure consists of one-dimensional polymer Cu^{II}cyclam–Cl–Cu^{I}–Cl–Cu^{II}cyclam. The coordination geometry of the Cu^{II} ion is an elongated octahedron while Cu^{I} ion is surrounded by three chlorine atoms in a trigonal geometry. The tetraazacyclotetradecane adopts the *trans*-III configuration. Compound **2** is monoclinic ($P2_1/n$), with $a = 10.3675(5)$ Å, $b = 11.2065(4)$ Å, $c = 9.4701(5)$ Å, $\beta = 116.93(0)°$, $V = 980.93(9)$ Å^3, $Z = 2$. The tetraprotonated cyclam H_4cyclam^{4+} has a (3,4,3,4)-B conformation. Copper(I) is tetrahedrally coordinated and two neighboring [$CuCl_4$] units share an edge to form isolated dimeric species [$Cu^{I}_2Cl_6$]. Compound **1** was tested to understand its influence on enzyme activity, immunomodulation as well as its toxicity and antiglycation potential. Effect of compound **1** was significant as immunomodulatory and inhibitory activity against β-glucuronidase enzyme ($IC_{50} = 0.55$ μM), but it did not affect significantly other biological activities tested.

Keywords Mixed valence · Copper(I/II) complexes · Halocuprates · Tetraazacyclotetradecane · X-ray structures · β-Glucuronidase · Enzyme inhibition

M. Lachkar · I. Halime · A. Bezgour
Engineering Laboratory of Organometallic and Molecular Materials, CNRST (URAC 19), Faculty of Sciences, University Sidi Mohamed Ben Abdellah, P.O. Box 1796, 30000 Fez, Atlas, Morocco

B. El Bali (✉)
Laboratory of Mineral Solid and Analytical Chemistry, 'LMSAC', Department of Chemistry, Faculty of Sciences, University Mohamed I, P.O. Box 717, 60000 Oujda, Morocco
e-mail: b.elbali@fso.ump.ma

M. Dusek · K. Fejfarova
Institute of Physics ASCR, v.v.i., Na Slovance 2, 182 21 Praha 8, Czech Republic

S. Siddiq
Dr. Panjwani Center for Molecular Medicine and Drug Research, International Center for Chemical and Biological Sciences, University of Karachi, Karachi 75270, Pakistan

B. P. Marasini · S. Noreen · A. Khan · S. Rasheed · M. I. Choudhary
H.E.J. Research Institute of Chemistry, International Center for Chemical and Biological Sciences, University of Karachi, Karachi 75270, Pakistan

M. I. Choudhary
Department of Chemistry, School of Science, King Saud University, Riyadh 11475, Saudi Arabia

Introduction

Macrocyclic ligands have been widely investigated because of their importance in coordination chemistry. Our work focuses the tetradentate macrocycle 1,4,8,11-tetrazacyclotetradecane (cyclam) (Scheme 1), an important azamacrocycle able to block four equatorial positions of a metal (Martell and Hancock, 1996; Wainwright, 1997; Lincoln, 1997; Meyer *et al.*, 1998; Lindoy, 1998). It forms complexes with a large range of metal ions, often with very high thermodynamic and kinetic stabilities (Liang and Sadler, 2004). It is also able to access unusual oxidation states of a metal centre (Melson, 1979; Yatsimirskii and Lampeka, 1985). In the last years, investigations of cyclam-derived ligands and their complexes have often

Scheme 1 Tetradentate macrocycle 1,4,8,11-tetraazacyclotetradecane (cyclam)

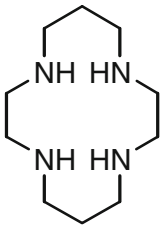

cyclam
$C_{10}H_{24}N_4$

been initiated for uses in medicine. Cyclam-based anti-HIV agents are more active in vivo in the form of metal ion complexes (Gerlach *et al.*, 2003; Liang *et al.*, 2002; Liang and Sadler, 2004). Indeed, cyclam offers an excellent binding environment for the Cu(II) ion, combining high thermodynamic stability and aqueous solubility (Moi *et al.*, 1985; Lukes *et al.*, 2001; Liang and Sadler, 2004). A large number of copper(II) coordination compounds have been reported as functional models for the active sites of copper proteins (Karlin and Tyelkar, 1993; Eichow and Marzili, 1994). One of the interesting features of such binuclear copper complexes is the existence of mixed valence species, exhibiting unusual oxidation states not normally achievable by mononuclear copper complexes (Gagne *et al.*, 1979). In the last two decades, halocuprate (I) and (II) compounds have been intensively studied (Subramanian and Hoffmann, 1992; Blake *et al.*, 1998; Graham *et al.*, 2000; Haddad and Willett, 2001; Arnby *et al.*, 2004; Nather and Jess, 2004). The coordination numbers and stereochemistries of Cu(I) and Cu(II) are also quite variable. In the cases of amines, copper(I) halides form mononuclear or multinuclear complexes in which its coordination number ranges from 2 to 4. Halides are established as good bridging ligands that can form halide-bridging polymetallic cluster complexes.

α-Chymotrypsin (EC 3.4.21.1), a protease, which is secreted from pancreas, catalyzes the breakdown polypeptide and proteins. At abnormal physiological cases, this enzyme not only digests proteins from foods, but also catalyzes the degradation of body's own tissues such as in cases of pancreatitis, cirrhosis (Beaud *et al.*, 2005). Phosphodiesterase (EC 3.1.4.1), catalyzes the release of nucleoside-5′-monophosphates from pyrophosphate and phosphodiester bonds. Coronary heart disease, venom poisoning, etc., are some disease condition arised due to the hyper-activated phosphodiesterase interfering many normal signalling processes (Mathieu *et al.*, 2000). Urease (EC 3.5.1.5) is a nickel containing metalloenzyme which catalyzes the hydrolysis of urea to ammonia and carbon dioxide. Urease is the causes of pathologies induced by *Helicobacter pylori*, thus allow them to survive at a low pH of the stomach, resulting peptic ulcers, apart from cancer as well. Urease is responsible for formation of stones and pathogenesis of urolithiasis, pyelnephritis and hepatic encephalopathy (Khan *et al.*, 2010). β-Glucuronidase (EC 3.2.1.31) is an exoglycosidase hydrolase enzyme that catalyzes the cleavage of glucuronosyl-*O*-bonds. It plays a major role in the generation of toxic and carcinogenic metabolites in the large intestine (Beaud *et al.*, 2005). The activity of this enzyme has been detected both in the intestinal tissues and intestinal bacteria. In the large intestine, bacterial species such as *Escherichia coli, Klebsiella* spp., *Clostridium* spp. and *Bacillus* spp. possess glucuronidase activity (Rod and Midtvedt, 1977; Leung *et al.*, 2001; Chouiter *et al.*, 2008) and generate toxic and carcinogenic materials which may promote tumours (Hawksworth and Draser, 1971; McBain and Macfarlane, 1998; Kim *et al.*, 1998). Many synthetic and natural compounds are used clinically to inhibit the activity of β-glucuronidase enzyme for the treatment of related diseases (Hua *et al.*, 1990). So, inhibitors of β-glucuronidase are of great pharmacological importance for better anti-tumour, antioxidant effects and reduction of systemic toxicity by excretion of toxic xenobiotics.

Immunocompetent cells are responsible to defense against infectious microorganisms releasing reactive oxygen species (ROS) along with other mechanisms. But hyperactive immunocompetent cells may be responsible to damage body's own tissues such as case in the rheumatoid arthritis. Many compounds have been reported, which affect the function of the immune system (Sell 1987; Mesaik *et al.* 2004; Wansi *et al.*, 2008). Immunomodulating agents, thus, got superiority in treating some abnormal physiological conditions, such as infections, cancer, organ transplantation, rheumatoid arthritis and systemic lupus erythromatosus (Bartlett *et al.*, 1991).

We report in this article on the synthesis and crystal structures of the two new complexes $[Cu^{II}cyclam][Cu^{I}Cl_3]$ **1** and $[H_4cyclam][Cu^{I}_2Cl_6]$ **2**. Due to lack in material, we, however, report only on the results of the activities from **1** in the inhibitions of the above-mentioned enzymes, which have been taken as target in many disease conditions as well as for immunomodulatory, antiglycation and cytotoxicity testing.

Experimental part

Synthesis

Copper(II) chloride dihydrate (0.85 g, 5 mmol) in water (5 ml) was added dropwise to a stirred acidic solution of cyclam (0.20 g, 1 mmol) in water (10 ml). A colour change was observed upon initial addition of copper(II) salt and the solution was heated at 60°C for 2 h. The resulting solution was allowed at room temperature, under air atmosphere, and after few days, dark violet crystals **1** first

appeared followed by yellow ones **2**. Crystals were collected when some residual solvent was still present and, then, washed with EtOH.

Characterizations

X-ray single crystal study

The X-ray diffraction data for **1** and **2** were collected on an Oxford Diffraction four-circles X-ray diffractometer XCALIBUR using graphite monochromatized Mo Kα radiation ($\lambda = 0.7173$ Å) and a SAPPHIRE CCD detector. The intensity data were corrected for Lorentz and polarization effects. A numeric analytical absorption correction was carried out with the program CrysAlis RED (Oxford Diffraction, 2005). The structures were solved with the Direct Methods procedure of SIR97 (Altomare *et al.*, 1999) and refined by a full-matrix least-squares technique based on F^2, Jana2006 (Petricek *et al.*, 2006). All non-hydrogen atoms were refined with anisotropic displacement parameters. Crystal and refinement data for the two new compounds are reported in Table 1. The atomic coordinates and equivalent thermal parameters are reported in Tables 2 and 3. Notice that the hydrogen atoms were localized from the difference Fourier maps and their coordinates were refined freely by constraining only O–H distances to 0.82(1) Å. The isotropic temperature parameters of hydrogen atoms were calculated as $1.2*U_{eq}$ of the parent atom. For plotting the structure DIAMOND program (Brandenburg, 2001) was used.

Selected bonds and angles values are summarized in Tables 4 and 5, respectively, for **1** and **2**.

Raman spectra were measured in a back scattering arrangement at ambient conditions by using a high-throughput holographic imaging spectrograph with volume transmission grating, holographic notch filter and thermo-electrically cooled CCD detector (Physics Spectra), and a resolution of 4 cm^{-1}. The spectrometer was regularly calibrated by using the neon lines. Ti^{3+}–sapphire laser pumped by an argon ion laser was tuned at 785 nm. The infrared measurements were performed in transmission geometry using a FTIR Biorad spectrometer FTS-40A with dynamic alignment and a spectral resolution of 2 cm^{-1} in the range 400–4,000 cm^{-1}. 0.2 mg sample per 200 mg KBr have been pressed into pellets. Electronic absorption spectra of solutions were measured by using a double-beam UV–Visible Camspec M550 spectrophotometer.

Table 1 Summary of crystal data, intensity measurement, and structure refinement for $[Cu^{II}cyclam][Cu^{I}Cl_3]$ **1** and $[H_4cyclam][Cu^{I}_2Cl_6]$ **2**

Chemical formula	$C_{20}H_{48}Cl_6Cu_4N_8$ (**1**)	$C_{10}H_{28}N_4{\cdot}Cl_6Cu_2$ (**2**)
M_r (g/mol)	867.6	544.16
Crystal system, space group	Orthorhombic, *Pccn*	Monoclinic, $P2_1/n$
Radiation, λ (Å)	Mo Kα, 0.71069	Mo Kα, 0.71069
a (Å), α (°)	22.6775(4), 90	10.3675(5), 90
b (Å), β (°)	22.8272(4), 90	11.2065(4),116.933(5)°
c (Å), γ (°)	12.5057(2), 90	9.4701(5), 90
V (Å^3)	6473.75 (19)	980.93 (9)
Z, *F*(000)	8, 3536	2, 552
Crystal size (mm^3)/μ (mm^{-1})	0.12 × 0.09 × 0.05 3.12	0.32 × 0.25 × 0.15 2.99
θ range for data collection (°)	2.5–26.5	2.4–26.5
Index ranges	$-28 < h < 28$ $-28 < k < 28$ $-15 < l < 15$	$-12 < h < 12$ $-14 < k < 14$ $-11 < l < 11$
Independent reflections	6,772	2,000
Reflections with $I_{obs} > 3\sigma(I_{obs})$	4,578	1,830
T_{min}/T_{max}	0.609/0.735	0.491/0.703
R_1/wR_2	0.019/0.039	0.018/0.080

$R_1 = \sum|F_o| - |F_c|/\sum|F_o|$, $wR_2 = \sqrt{\frac{\sum\left(w\left(|F_o|^2-|F_c|^2\right)\right)^2}{\sum\left(w\cdot|F_o|^2\right)^2}}$

Biological activities

β-Glucuronidase inhibition assay

β-Glucuronidase activity was determined by the spectrophotometric method measuring the absorbance at 405 nm of *p*-nitrophenol formed from the substrate. The total reaction volume is 250 µl. The reaction mixture contained 185 µl of 0.1 M acetate buffer, 5 µl of test compound solution, 10 µl of enzyme solution was incubated at 37°C for 30 min. The plates were read on a multiplate reader (SpectraMax plus 384) at 405 nm after the addition of 50 µl of 0.4 mM *p*-nitrophenyl-β-D-glucuronide (Riaz *et al.*, 2003).

Urease inhibition assay

Reaction mixtures comprising 1 U of urease enzyme (Jack bean) solution and 55 µl of buffers containing 100 mM urea were incubated with 5 µl of test compounds (0.5 mM) at 30°C for 15 min in 96-well plates. Urease activity was determined by measuring ammonia production using the indophenol method. Briefly, 45 µl each of phenol reagent and 70 µl of alkali reagent were added to each well. The increasing absorbance at 630 nm was measured after 50 min, using a microplate reader (Khan *et al.*, 2010).

Table 2 Fractional atomic coordinates and isotropic or equivalent isotropic displacement parameters (Å^2) for **1**

Atom	*x*	*y*	*z*	U_{iso}/U_{eq}
Cu1	0.852547 (10)	−0.094482 (9)	0.019130 (18)	0.01190 (7)
Cu2	0.598589 (10)	0.146120 (10)	0.013550 (18)	0.01230 (7)
Cu3	0.515371 (11)	0.312539 (10)	0.05422 (2)	0.01967 (8)
Cu4	0.690636 (11)	−0.011856 (10)	0.08650 (2)	0.02007 (8)
Cl1	0.60448 (2)	0.02237 (2)	0.02495 (4)	0.02037 (15)
Cl2	0.47739 (2)	0.39354 (2)	−0.02120 (4)	0.01737 (14)
Cl3	0.73780 (2)	0.03689 (2)	0.22232 (4)	0.01839 (15)
Cl4	0.59800 (2)	0.270047 (19)	−0.00661 (4)	0.01768 (14)
Cl5	0.46734 (2)	0.27283 (2)	0.19831 (4)	0.02030 (15)
Cl6	0.72942 (2)	−0.09558 (2)	0.02316 (4)	0.01938 (15)
N1	0.53693 (7)	0.15387 (7)	0.12750 (13)	0.0123 (5)
N2	0.65761 (7)	0.14956 (6)	0.13375 (12)	0.0117 (5)
N3	0.85336 (7)	−0.16767 (7)	−0.07108 (12)	0.0124 (5)
N4	0.85114 (7)	−0.05024 (7)	−0.12047 (12)	0.0123 (5)
N5	0.85713 (7)	−0.13915 (7)	0.15924 (12)	0.0140 (5)
N6	0.54014 (7)	0.14283 (7)	−0.10776 (12)	0.0143 (5)
N7	0.66129 (7)	0.13616 (7)	−0.10097 (13)	0.0133 (5)
C1	0.62563 (8)	0.17131 (8)	0.22918 (15)	0.0161 (6)
C2	0.83376 (9)	−0.14985 (8)	−0.17941 (15)	0.0169 (6)
N8	0.85494 (7)	−0.02173 (7)	0.10980 (12)	0.0131 (5)
C3	0.56562 (8)	0.14284 (8)	0.23185 (15)	0.0160 (6)
C4	0.82503 (9)	−0.19513 (8)	0.16812 (16)	0.0206 (7)
C5	0.57185 (8)	0.11914 (8)	−0.20144 (15)	0.0177 (6)
C6	0.71244 (8)	0.18263 (8)	0.11261 (15)	0.0155 (6)
C7	0.86540 (8)	−0.09312 (8)	−0.20461 (15)	0.0163 (6)
C8	0.63228 (8)	0.14662 (9)	−0.20521 (15)	0.0186 (7)
C9	0.84066 (8)	−0.09663 (8)	0.24366 (15)	0.0168 (6)
C10	0.87338 (8)	0.04663 (8)	−0.04262 (15)	0.0168 (6)
C11	0.84256 (9)	−0.23764 (8)	0.07964 (15)	0.0216 (7)
C12	0.87180 (8)	−0.03957 (8)	0.21976 (15)	0.0154 (6)
C13	0.48171 (8)	0.12049 (8)	0.11436 (15)	0.0172 (6)
C14	0.71716 (8)	0.16814 (8)	−0.08943 (16)	0.0186 (6)
C15	0.45143 (8)	0.13398 (9)	0.00967 (15)	0.0209 (7)
C16	0.82195 (9)	−0.21951 (8)	−0.03098 (15)	0.0184 (6)
C17	0.88918 (8)	0.00233 (8)	−0.12711 (16)	0.0160 (6)
C18	0.74600 (8)	0.15769 (8)	0.01850 (15)	0.0172 (6)
C19	0.48425 (8)	0.11125 (9)	−0.08795 (16)	0.0209 (7)
C20	0.89020 (8)	0.02849 (8)	0.07015 (15)	0.0160 (6)
H11	0.621151	0.213042	0.224327	0.0193
H12	0.647129	0.160915	0.292529	0.0193
H21	0.791969	−0.14317	−0.178895	0.0203
H22	0.84511	−0.179263	−0.230281	0.0203
H31	0.570035	0.101409	0.24229	0.0192
H32	0.542457	0.160076	0.287881	0.0192
H41	0.783376	−0.187904	0.164668	0.0247
H42	0.833004	−0.212569	0.236469	0.0247
H51	0.55064	0.128839	−0.265479	0.0212
H52	0.575668	0.077441	−0.194315	0.0212
H61	0.737038	0.181814	0.175067	0.0186
H62	0.702982	0.22292	0.098832	0.0186

Table 2 continued

Atom	*x*	*y*	*z*	U_{iso}/U_{eq}
H71	0.907177	−0.099866	−0.205697	0.0195
H72	0.852218	−0.078533	−0.272534	0.0195
H81	0.655019	0.128667	−0.261059	0.0223
H82	0.628517	0.188009	−0.216973	0.0223
H91	0.853298	−0.111117	0.311993	0.0201
H92	0.798785	−0.090506	0.242426	0.0201
H101	0.831833	0.054548	−0.045551	0.0201
H102	0.891564	0.083481	−0.059347	0.0201
H111	0.827597	−0.275953	0.095957	0.0259
H112	0.884624	−0.242373	0.079352	0.0259
H121	0.859113	−0.010194	0.269648	0.0185
H122	0.913679	−0.045434	0.223085	0.0185
H131	0.455524	0.129236	0.172525	0.0206
H132	0.490026	0.079313	0.118289	0.0206
H141	0.710237	0.20931	−0.09886	0.0223
H142	0.74374	0.156578	−0.145318	0.0223
H151	0.445923	0.175525	0.003228	0.0251
H152	0.412253	0.118062	0.010585	0.0251
H161	0.827366	−0.2515	−0.079842	0.0221
H162	0.780371	−0.211666	−0.029295	0.0221
H171	0.885225	0.019814	−0.196558	0.0192
H172	0.929697	−0.009001	−0.118865	0.0192
H181	0.785282	0.173369	0.017835	0.0206
H182	0.751818	0.116423	0.028869	0.0206
H191	0.492214	0.070226	−0.079205	0.0251
H192	0.459344	0.114352	−0.149768	0.0251
H201	0.931332	0.018618	0.072231	0.0192
H202	0.885385	0.061205	0.117589	0.0192
H1	0.5264 (8)	0.1903 (3)	0.1231 (15)	0.0148
H2	0.6684 (8)	0.1138 (3)	0.1463 (14)	0.014
H3	0.8907 (3)	−0.1753 (8)	−0.0757 (15)	0.0149
H4	0.8149 (3)	−0.0392 (8)	−0.1307 (15)	0.0147
H5	0.8950 (3)	−0.1445 (8)	0.1618 (15)	0.0168
H6	0.5302 (8)	0.1784 (4)	−0.1242 (15)	0.0171
H7	0.6698 (8)	0.0994 (3)	−0.0940 (15)	0.016
H8	0.8183 (3)	−0.0107 (8)	0.1114 (15)	0.0157

α-Chymotrypsin inhibition assay

α-Chymotrypsin (12 U/ml), prepared in Tris–HCl buffer pH 7.6 containing 10 mM $CaCl_2$, was incubated with various concentrations of test compounds for 25 min at 30°C. Then *N*-succinyl-phenylalanine-*p*-nitroanilide, (0.4 mM final) was added and the change in absorbance due to released *p*-nitroaniline was continuously monitored at 410 nm until a significant colour change. The final DMSO concentration was maintained up to 7% (Choudhary *et al.*, 2011).

Phosphodiesterase inhibition assay

Snake venom phosphodiesterase activity was performed in 33 mM Tris–HC1 buffer with 30 mM Mg acetate buffer pH 8.8. The buffer, various concentrations of test compounds and enzyme (0.742 mU/well) were incubated at 37°C for 30 min. The plates were read on a multiplate reader, SpectraMax plus 384 (Molecular Device, CA, USA) at 410 nm after the addition of 0.33 mM bis-(*p*-nitropheny1) phosphate (Ahmad et al., 2003).

Table 3 Fractional atomic coordinates and isotropic or equivalent isotropic displacement parameters (Å^2) for **2**

Atom	*x*	*y*	*z*	U_{iso}/U_{eq}
Cu1	0.48551 (3)	0.48308 (3)	0.33442 (3)	0.01656 (14)
Cl1	0.69755 (5)	0.46262 (4)	0.29877 (6)	0.01133 (18)
Cl2	0.27803 (5)	0.45399 (4)	0.09228 (6)	0.01392 (19)
Cl3	0.48833 (5)	0.66252 (4)	0.46591 (6)	0.0167 (2)
N1	0.3533 (2)	0.99612 (15)	0.1712 (2)	0.0127 (6)
N2	0.58022 (18)	0.76876 (15)	−0.02070 (19)	0.0136 (6)
C1	0.4621 (2)	0.90445 (19)	0.1807 (2)	0.0165 (8)
C2	0.3882 (2)	0.79514 (18)	0.0773 (2)	0.0140 (7)
C3	0.4962 (2)	0.71277 (18)	0.0581 (2)	0.0150 (8)
C4	0.4907 (2)	0.82249 (19)	−0.1832 (2)	0.0134 (7)
C5	0.5830 (2)	0.88584 (18)	−0.2492 (2)	0.0137 (7)
H1m	0.299778	0.967273	0.212102	0.0152
H1n	0.292114	1.008159	0.072533	0.0152
H2m	0.638977	0.822482	0.041745	0.0163
H2n	0.640026	0.716579	−0.025962	0.0163
H1a	0.517579	0.879676	0.288706	0.0198
H1b	0.52796	0.939139	0.146529	0.0198
H2a	0.337077	0.751553	0.12354	0.0169
H2b	0.317129	0.821259	−0.025159	0.0169
H3a	0.447058	0.642756	0.000421	0.018
H3b	0.562578	0.681549	0.159691	0.018
H4a	0.422147	0.877787	−0.178236	0.016
H4b	0.434285	0.76103	−0.255366	0.016
H5a	0.659271	0.833678	−0.241702	0.0164
H5b	0.526667	0.897433	−0.361152	0.0164

Antigylcation assay

Triplicate samples of BSA, 10 mg/ml, 14 mM MGO, 0.1 M phosphate buffer (pH 7.4) containing NaN_3 (30 mM) were incubated under sterile conditions, in 96-well plate at 37°C for 9 days. After 9 days of incubation, each sample was examined for the development of specific fluorescence (excitation, 330 nm and emission, 440 nm), against sample blank on a microtitre plate spectrophotometer (SpectraMax M2, CA, USA) (Rahbar and Figarola, 2003). The percent inhibition was calculated by using the following formula:

$$\% \text{ Inhibition} = (1 - \text{Fluorescence of test sample} / \text{Fluorescence of the control group}) \times 100$$

Cytotoxicity assay

Cytotoxicity of compounds was evaluated by using the MTT (3-[4,5-dimethylthiazole-2-yl]-2,5-diphenyl-tetrazolium bromide) colorimetric assay (Mosmann, 1983). Both CC1 and PC-3 cells were cultured in Dulbecco's Modified Eagle's Medium, supplemented with 5% of fetal bovine serum (FBS), 100 IU/ml of penicillin and 100 µg/ml of streptomycin in 75 cm^2 flasks, and kept in 5% CO_2 incubator at 37°C. Exponentially growing cells 1×10^4 cells/well were maintained into each well of 96-well plates. After overnight incubation, medium was removed and 200 µl of fresh medium was added with different concentrations of compounds. After 48 h, 50 µl MTT (2 mg/ml)

Table 4 Selected bonds and angles values in **1**

Cu1–Cl2^{i}	2.8444 (5)	N5–C9	1.482 (2)
Cu1–Cl6	2.7927 (5)	N5–H5	0.868 (7)
Cu2–Cl1	2.8317 (5)	N6–C5	1.477 (2)
Cu2–Cl4	2.8401 (5)	N6–C19	1.479 (3)
Cu3–Cl2	2.2473 (5)	N6–H6	0.867 (10)
Cu3–Cl4	2.2429 (5)	N7–C8	1.480 (3)
Cu3–Cl5	2.2925 (6)	N7–C14	1.469 (2)
Cu4–Cl1	2.2406 (5)	N7–H7	0.865 (8)
Cu4–Cl3	2.2950 (5)	N8–C12	1.484 (2)
Cu4–Cl6	2.2481 (5)	N8–C20	1.483 (2)
N1–C3	1.480 (2)	N8–H8	0.869 (9)
N1–C13	1.475 (2)	C1–C3	1.508 (3)
N1–H1	0.867 (9)	C2–C7	1.514 (3)
N2–C1	1.482 (2)	C4–C11	1.525 (3)
N2–C6	1.478 (2)	C5–C8	1.508 (3)
N2–H2	0.867 (10)	C6–C18	1.513 (3)
N3–C2	1.483 (2)	C9–C12	1.512 (3)
N3–C16	1.469 (2)	C10–C17	1.506 (3)
N3–H3	0.868 (8)	C10–C20	1.518 (3)
N4–C7	1.473 (2)	C11–C16	1.518 (3)
N4–C17	1.480 (2)	C13–C15	1.510 (3)
N4–H4	0.868 (9)	C14–C18	1.519 (3)
N5–C4	1.475 (3)	C15–C19	1.521 (3)

Symmetry codes: (i) $x + 1/2, y - 1/2, -z$; (ii) $x - 1/2, y + 1/2, -z$

Table 5 Selected bonds and angles values in **2**

Cu1–Cl1	2.3815 (7)	C1–H1a	0.96
Cu1–Cl2	2.3501 (5)	C1–H1b	0.96
Cu1–Cl3	2.3585 (6)	C2–C3	1.524 (3)
Cu1–Cl3^{i}	2.4180 (6)	C2–H2a	0.96
N1–C1	1.498 (3)	C2–H2b	0.96
N1–C5^{ii}	1.513 (3)	C3–H3a	0.96
N1–H1m	0.87	C3–H3b	0.96
N1–H1n	0.87	C4–C5	1.533 (4)
N2–C3	1.516 (3)	C4–H4a	0.96
N2–C4	1.516 (2)	C4–H4b	0.96
N2–H2m	0.87	C5–H5a	0.96
N2–H2n	0.87	C5–H5b	0.96
C1–C2	1.539 (3)		

Symmetry codes: (i) $-x + 1, -y + 1, -z + 1$; (ii) $-x + 1, -y + 2, -z$

was added to each well and incubated further for 4 h. Subsequently, 100 µl of DMSO was added to each well and the absorbance was measured at 570 nm (for PC-3) or 540 nm (for CC1), using a microplate reader (SpectraMax plus 384).

Immunomodulatory activity (oxidative burst study)

Luminol-enhanced chemiluminescence assay was performed as described by Helfand *et al.* (1982). 25 µl of 1:50 diluted whole blood in HBSS with Ca^{2+} and Mg^{2+} Sigma-Aldrich (Steinheim, Germany) was incubated with 25 µl of serially diluted compound Cu Cyclam with concentration ranges between 1 and 100 µg/ml. Control wells contain HBSS with Ca^{2+} and Mg^{2+} and whole blood but no compound. Test was performed in white 96-well plates Corning (NY, USA), which was incubated at 37°C for 20 min in the thermostated chamber of the luminometer. Opsonized zymosan-A (*Saccharomyces cerevisiae* origin) 25 µl, followed by 25 µl luminol (7×10^{-5} M) Alfaaesar (Karlsruhe) along with HBSS were added to each well to obtain a 100-µl volume/well. The luminometer results were monitored as chemiluminescence reading, Relative Light Unit (RLU).

$$\% \text{ Inhibition} = 100 - (\text{RLU of test sample}/\text{RLU of the control}) \times 100$$

Assay for nitric oxide immunomodulation

The mouse macrophage cell line J774.2 was cultured in 75 cc flasks that contained 10% fetal bovine serum supplemented with streptomycin/penicillin 1%. Flasks were kept at 37°C in atmosphere of humidified air containing 5% CO_2. Then, cells were seeded in 24-well plate (10^6 cells/ml) and nitric oxide synthase (NOS-2) in macrophages was induced by 20 µg/ml *E. coli* lipopolysaccharide (LPS). The test compound was given at concentration of 25 µg/ml soon after LPS stimulation and it was again incubated at 37°C in 5% CO_2 and 95% air. The cell culture supernatant was collected after 48 h for further analysis. Nitrite accumulation in J774.2 cell culture supernatant was measured using the Griess method described previously (Andrade *et al.*, 2005). Briefly, 50 µl of 1% sulphanilamide in 2.5% phosphoric acid, followed by 50 µl of 0.1% naphthyl-ethylene diamine dihydrochloride in 2.5% phosphoric acid was added to 50 µl of culture medium. After 10 min of incubation at room temperature in dark the absorbance at 550 nm was read. Micromolar concentrations of nitrite were calculated from standard curve constructed with sodium nitrite which was used as reference compound.

Statistical analysis

All reactions were performed in triplicate in a final volume of 200 µl. The results were processed by using SoftMax Pro 4.8 software (Molecular Devices, CA, USA) and then by MS Excel. The percentage of inhibition was calculated by the following formula:

$$\% \text{ Inhibition} = 100 - (\text{OD of test sample}/\text{OD of the control}) \times 100$$

Results were presented as means ± standard error mean from triplicate ($n = 3$) observation. IC_{50} values were determined by using EZ-FIT, Enzyme kinetics software by Perrella Scientific, Inc. USA.

Results and discussions

Crystal structure of **1**

The title compound is a mixed-valence Cu(I)–Cu(II) complex which contains a 1,4,8,11-tetrazacyclotetradecane molecule bonded to the central copper(II) atom and two almost planar $[Cu(I)Cl(3)]^{2-}$ moieties. The building block $[Cu^{II}cyclam]$ is linked by $[Cu^{I}Cl_3]^{2-}$ to form a zigzag channel $\{[Cu^{II}cyclam][Cu^{I}Cl_3]\}_n$ as shown in Fig. 1.

The Cu–N bond lengths (2.004(5)–2.031(5) Å) are in the range expected for a Cu^{II} ion coordinated in a cyclam cavity (Studer *et al.*, 1989; Orpen *et al.*, 1989). The coordination sphere of the Cu^{2+} is completed by two axially bonded chlorine atoms of two $CuCl_3^{2-}$ moieties. Figure 2 reports the coordination scheme of Cu^{I} and Cu^{II} in the title compound. The axial bonds $Cu^{II}(1)$–Cl(2) and $Cu^{II}(1)$–Cl(6) are, respectively, 2.844(5) and 2.793(5) Å, while $Cu^{II}(2)$–Cl(1) and $Cu^{II}(2)$–Cl(4) are 2.832(5) and 2.840(5) Å. The apical angles Cl(2)–$Cu^{II}(1)$–Cl(6) and Cl(1)–$Cu^{II}(2)$–Cl(4) are, respectively, 173.77(2)° and 176.72(2)°. The geometry around the copper(II) centre may be described as a distorted octahedron as usually observed for the Jahn–Teller distorsion of Cu(II). Cl(2) and Cl(4), from one side, and Cl(1) and Cl(6), from the other side, are shared between the Cu^{I} and Cu^{II} polyhedrons; this results in shorter Cu(3)–Cl(n) ($n = 2$, 4), respectively, 2.243(5) and 2.247(5) Å, and $Cu^{I}(4)$–Cl(n) ($n = 1$, 6), 2.248(5) and 2.241(5) Å. Comparatively, the remaining distances $Cu^{I}(3)$–Cl(5) and $Cu^{I}(4)$–Cl(3) are longer, respectively, 2.292(5) and 2.295(5) Å. Short Cu^{II}–Cu^{I} distance in $[Cu^{II}cyclam][Cu^{I}Cl_3]$ is 4.2129(3) Å. The spin holders (Cu^{2+}, $3d^9$) are isolated in the structure avoiding all possible magnetic interactions in the complex.

The 14-membered macrocycle adopts the preferred *trans*-III configuration. In such configuration, the two six-membered chelating rings are in the chair form and the two

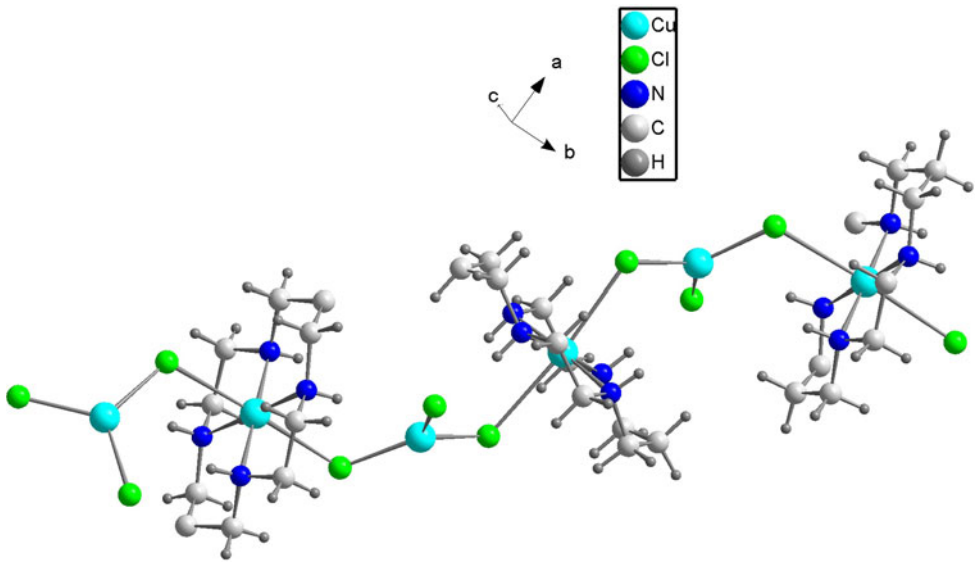

Fig. 1 Zigzag channels $\{[Cu^{II}cyclam][Cu^{I}Cl_3]\}_n$ in the structure of **1**

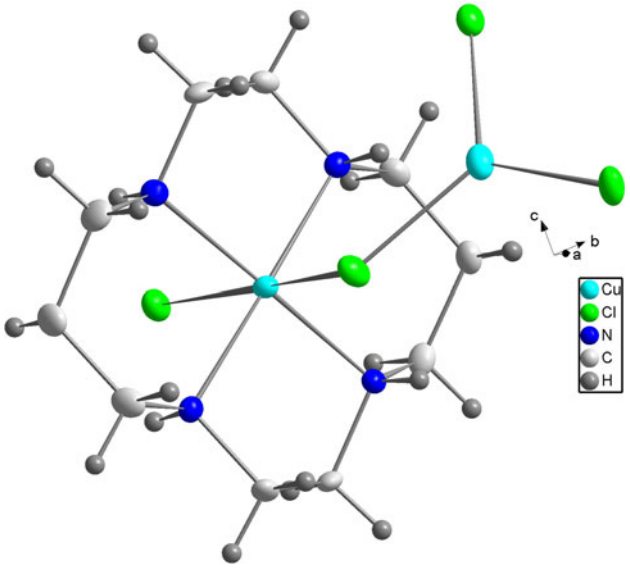

Fig. 2 Coordination scheme of Cu^{I} and Cu^{II} in **1**

five-member rings in the gauche form (the two NH hydrogens orient to a side opposite that of the other two). This configuration is thermodynamically the most stable form according to Bosnich *et al.* (1965). As expected, the N–Cu–N angles of the five-membered chelating rings are acute while those of the six-membered chelates are obtuse.

The IR spectrum of $[Cu^{II}cyclam][Cu^{I}Cl_3]$ exhibits broad band at 3,415 cm^{-1} associated with the water molecules, one strong band at 3,180 cm^{-1}, attributable to the ν(N–H) vibrations of the macrocycle, strong bands between 2,860 and 2,960 cm^{-1}, attributable to the ν(C–H) vibrations of aliphatic C–H groups. The bands at about 1,464 and 1,434 cm^{-1} can be ascribed to the δ(C–H) asymmetric and symmetric modes, respectively. However, these bands are less intense than those observed for the free cyclam (Diaz *et al.*, 1997). The band at 1,126 cm^{-1} is due to a ν(C–N) mode. The medium band at 1,065 cm^{-1} can be attributed to the ν(C–C) mode. The band at 1,004 cm^{-1} should correspond to the δ(N–H) mode (Lien-Vien *et al.*, 1991). The band at 436 cm^{-1} can be assigned to the Cu–N (cyclam) mode (Diaz *et al.*, 1997; Nakamoto, 1997).

A spectroscopic study of complex **1** shows that the structure in the crystal, established by X-ray, is preserved in solution. The UV–visible spectrum of $[Cu^{II}cyclam][Cu^{I}Cl_3]$ exhibits one absorption at 508 nm with a low ε value (15.5 mol^{-1} l cm^{-1}). The low molar absorptivity of less than 100 mol^{-1} l cm^{-1} is consistent with a pseudo-octahedral solution geometry (Boswell *et al.*, 2004). The weak band observed at 508 nm is a ligand field copper(II) transition. It has been well established that in mixed valence copper(II)–copper(I) complexes, an intervalence transfer transition (I.T.) [copper(I)–copper(II) → copper(II)–copper(I)] occurs in the near I. R. region and is solvent dependent (Robin and Day, 1967). Complex **1** shows this I.T. band at ca. 803 nm in H_2O.

Crystal structure of **2**

The crystal structure of $[H_4cyclam][Cu_2Cl_6]$ might be described in terms of discrete dinuclear $[Cu^{I}_2Cl_6]^{4-}$ and tetraprotonated $[H_4cyclam]^{4+}$ entities. A fragment of the structure of **2** is reported in Fig. 3. The dimeric anion $[Cu^{I}_2Cl_6]^{4-}$ consists of two edge sharing $[CuCl_4]$ tetrahedrons. Its charge balances the tetraprotonated cyclam entity, which means the presence of Cu^{+} in the title compound. $[CuCl_4]$ being a distorted tetrahedron, the four bonds distances Cu–Cl range from 2.381(2) to 2.418(1) Å. List of bonds (Cu–Cl) and angles (Cl–Cu–Cl) in the tetrahedron are listed in Table 5.

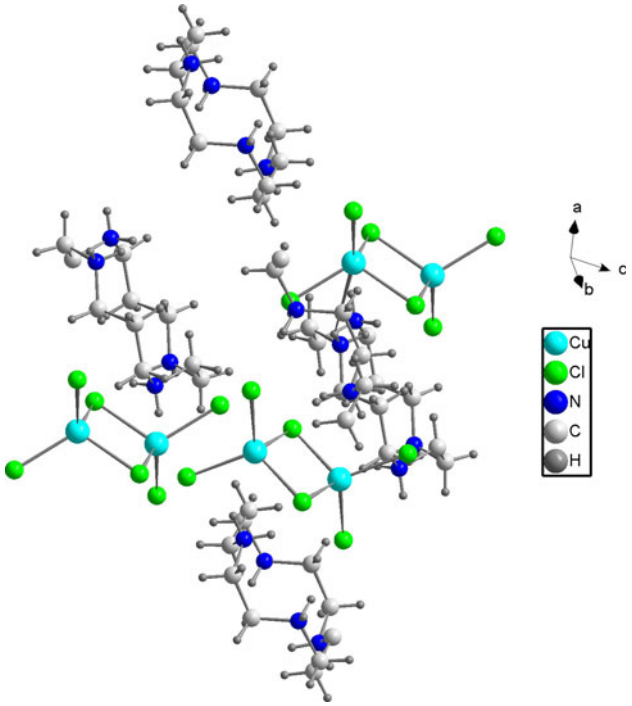

Fig. 3 A fragment of the crystal structure of **2** with dimmers $[Cu_2^1Cl_6]^{4-}$ and $[H_4cyclam]^{4+}$ entities

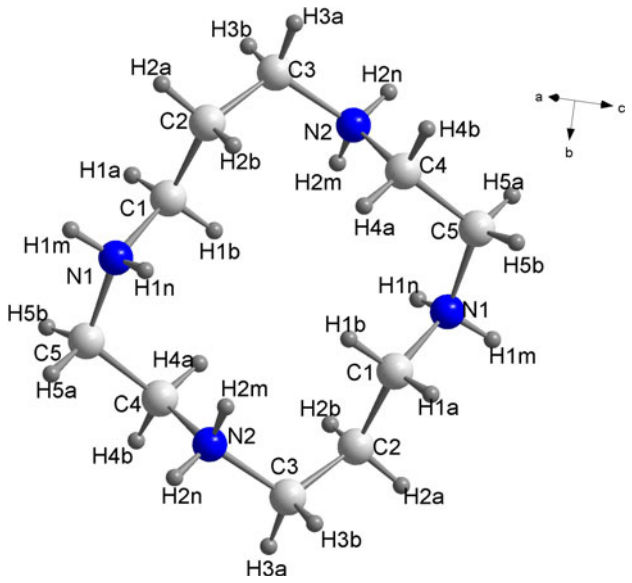

Fig. 4 (3,4,3,4)-B conformation of the $H_4cyclam^{4+}$ in **2**

The distance Cu···Cu inside the dimmer is 3.036 Å, shorter than the corresponding value in **1** (4.2129(3) Å). A network of weak H-bonds interactions between the Cl corners from $[Cu_2Cl_6]$ and the ammonium groups of the tetraazamacrocycle might promote the cohesion in the crystal. Strong N–H···Cl interactions range between 2.292 and 2.342 Å.

The conformation of the tetraprotonated macrocycle resembles a rectangle (Fig. 4), at the corner of which four CH_2 groups are situated and the four nitrogen atoms are essentially coplanar, so the $H_4cyclam^{4+}$ cation has a (3,4,3,4)-B conformation (Hancock *et al.*, 1996). In spite of unfavourable electrostatic interactions, the endo (3,4,3,4)-B conformation is stabilized by extensive hydrogen bonding with the Cu_2Cl_6 groups.

The infrared spectrum of complex **2** exhibits one strong bands at 3,182 cm^{-1}, attributable to the ν(N–H) vibrations of the macrocycle, two bands between 2,850 and 2,950 cm^{-1}, attributable to the ν(C–H) vibrations of aliphatic C–H groups as well as the various bands characteristic of C–H and C–N groups (850–1,500 cm^{-1}).

Biological activities

Due to a lack of material, we did test only the compound **1**. Although it failed to show any inhibition against α-chymotrypsin, and phosphodiesterase enzymes, it showed a weak inhibition for urease and strong for β-glucuronidase enzyme (Table 6). The IC_{50} (0.55 ± 0.01 μM) of this compound against β-glucuronidase indicates very potent inhibitor than the standard, D-saccharic acid 1,4-lactone (IC_{50} 48.4 ± 1.3 μM). Due to availability, we tested this Cu^{2+} complex only on β-glucuronidase of bacterial source and in the literature the the Cu^{2+} complex found to inhibit mammalian β-glucuronidase as well (Fernley, 1962). Also, we were unable to set the in vivo model, however, the bacterial cell based in vivo model for inhibition of β-glucuronidase had shown equal or better inhibitory effect then the pure enzyme. And the inhibitor of β-glucuronidase in mice had shown to reduce toxic effects generated by β-glucuronidase for cancer therapeutics (Wallace *et al.*, 2011).

To explore further their therapeutic potential, we also checked this compound for various biological activities, i.e., antiglycation, immunomodulatory and cytotoxicity (against PC-3 and CC1 cell line) (Table 7). This compound did not show any antiglycation potential. Immunomodulatory activity of the compound **1** was done by chemiluminescence assay for ROS inhibition and NO_2 assay for nitric oxide inhibition. The compound showed significant inhibitory activity against ROS inhibition (IC_{50} ± SEM = 6.3 ± 0.8 μM) as compared to the standard, Ibuprofen (IC_{50} ± SEM = 11.8 ± 1.8 μM). ROS generation in cells is reduced either by inhibiting generation of superoxide anion or by the dismutation of superoxide anion into oxygen and peroxide. The copper(II) complexes might acted as the dismutation agent to convert superoxide anion into oxygen and peroxide (Diaz *et al.*, 1997). It showed moderated activity for NO_2 inhibition that is 31.3% at 25 μg/ml. In case of cytotoxicity, the compound showed 50% growth inhibition at concentration of 34.5 ± 2.8 μM for CC1 cell line but did not show toxicity for PC-3 cell line.

Table 6 Enzymes inhibitory activity of tested compound **1**

Compound code	(IC_{50} ± SEM) μM			
	α-Chymotrypsin	β-Glucuronidase	Urease	Phosphodiesterase
CuCyclam	NA	0.55 ± 0.01	326.83 ± 1.28	NA
Standard	Chymostatin	D-Saccharic acid 1–4 lactone	Thiourea	EDTA
	5.7 ± 0.1	48.4 ± 1.3	21 ± 0.01	74 ± 1.25

NA not active, i.e., less than 50% of inhibition at 500 μM; *SEM* standard error of mean

Table 7 Other biological activities of tested compound **1**

Compound code	(IC_{50} ± SEM) μM				
	Antiglycation	ROS	% Inhibition RNS (25 μg/ml)	Cytotoxicity (CC1)	Cytotoxicity (PC-3)
CuCyclam	NA	6.3 ± 0.8	31.3%	34.5 ± 2.8	NA
Standard	Rutin	Ibuprofen	NO	NO	Doxorobincin
	294.5 ± 1.5	11.8 ± 1.8			0.9 ± 0.1

NA not active, *NR* not optimized, *SEM* standard error of mean

Conclusions

Two new halocuprates complexes $[Cu^{II}cyclam][Cu^{I}Cl_3]$ and $[H_4cyclam][Cu^{I}_2Cl_6]$ have been synthesized and characterized by single-crystal X-ray structure determination, IR and UV–Visible spectroscopies. $[Cu^{II}cyclam][Cu^{I}Cl_3]$ consists of Cu^{2+} macrocyclic units $[Cu^{II}cyclam]^{2+}$, which are bridged by $Cu^{I}Cl_3{}^{2-}$ moieties leading to 1D coordination polymer. The geometry around the copper(I) centre is trigonal planar, while that of copper(II) centre is tetragonally distorted octahedral. The cyclam adopts its preferred configuration, namely the *trans*-III. In the doubly complex salt $[H_4cyclam][Cu^{I}_2Cl_6]$, each copper(I) in the dimmer species $[Cu^{I}_2Cl_6]$ is in a distorted tetrahedral geometry. The two copper are bridged by two chloride ions. The tetraprotonated cyclam $[H_4cyclam]^{4+}$ has a (3,4,3,4)-B conformation. Compound **1** showed the inhibitory effect against β-glucuronidase enzyme, which is highly expressed in tumour cell. Also, it showed immune modulation. These results suggest that compound **1** could be an inhibitor of ROS, anti-inflammatory and tumour suppressive agent.

Acknowledgments This work was financially supported by the CNRST (URAC 19). Universities Sidi Mohamed Ben Abdellah (Fès) and Mohammed 1er (Oujda) are gratefully acknowledged.

References

Ahmad VU, Abbasi MA, Hussain H, Akhtar MN, Farooq U, Fatima N, Choudhary MI (2003) Phenolic glycosides from *Symplocos racemosa*: natural inhibitors of phosphodiesterase I. Phytochemistry 63:217–220

Altomare A, Burla MC, Camalli M, Cascarano GL, Giacovazzo C, Guagliardi A, Moliterni AGG, Polidori G, Spagna R (1999) SIR97. J Appl Crystallogr 32:115–119

Andrade MA, Lucas MS, Arellano JLP, Barreto CP, Valladares B, Espinoza E, Muro A (2005) Increased rat alveolar macrophage expression of functional iNOS induced by a *Dirofilaria immitis* immunoglobulin superfamily protein. Nitric Oxide 13:217–225

Arnby CH, Jagner S, Dance I (2004) Questions for crystal engineering of halocuprate complexes: concepts for a difficult system. CrystEngComm 6(46):257–275

Bartlett RR, Dimitrijevic M, Mattar T, Zielinski T, Germann T, Rude E, Thoenes GH, Kuchle CC, Schorlemmer HU, Bremer E, Leflunomide HWA (1991) A novel immunomodulating compound for the treatment of autoimmune disorders and reactions leading to transplantation rejection. Agents Actions 32:10–21

Beaud D, Tailliez P, Mondoloni JA (2005) Genetic characterization of the β-glucuronidase enzyme from a human intestinal bacterium *Ruminococcus gnavus*. Microbiology 151:2323–2330

Blake AJ, Brooks NR, Champness NR, Hanton LR, Hubberstey P, Schroder M (1998) Copper(I) halide supramolecular networks linked by N-heterocyclic donor bridging ligands. Pure Appl Chem 70:2351–2357

Bosnich B, Poon CK, Tobe M (1965) Complexes of cobalt(III) with a tetradentate secondary amine. Inorg Chem 4:1102–1108

Boswell CA, Sun X, Niu W, Weisman GR, Wong EH, Rheingold AL, Anderson CJ (2004) Comparative in vivo stability of cross-bridged and conventional tetraazamacrocyclic complexes. J Med Chem 47:1465–1474

Brandenburg K (2001) DIAMOND, Crystal impact GbR, Bonn, Germany, Version 2.1 e

Choudhary MI, Adhikari A, Rasheed S, Marasini BP, Hussain N, Kaleem WA, Atta-ur-Rahman (2011) Cyclopeptide alkaloids of *Ziziphus oxyphylla* Edgw as novel inhibitors of α-glucosidase enzyme and protein glycation. Phytochem Lett 4(4):404–406

Chouiter R, Roy I, Bucke C (2008) Optimisation of β-glucuronidase production from a newly isolated *Ganoderma applanatum*. J Mol Catal B: Enzym 50(2–4):114–120

Diaz GF, Clavijo CRE, Campos-Vallette MM, Saavedra SM, Diez D, Munoz R (1997) Specular reflectance infrared spectra of the macrocycles cyclam and cyclamdione and their Cu(II) complexes deposited onto a smooth copper surface. Vib Spectrosc 15(2):201–209

Eichow GL, Marzili LG (1994) Advances in inorganic biochemistry. Prentice Hall, Englewood Cliffs, NJ

Fernley HN (1962) Effects of some heavy-metal ions on purified mammalian β-glucuronidase. Biochem J 82:500–510
Gagne RR, Koval CA, Smith TJ, Cimolino MC (1979) Binuclear complexes of macrocyclic ligands. J Am Chem Soc 101:4571–4580
Gerlach LO, Jakobsen JS, Jensen KP, Rosenkilde MR, Skerlj RT, Ryde U, Bridger GJ, Schwartz TW (2003) Metal-ion enhanced ligand binding of AMD3100 to the CXCR4 receptor. Biochemistry 42:710–717
Graham PM, Pike RD, Sabat M, Bailey RD, Pennington WT (2000) Coordination polymers of copper (I) halides. Inorg Chem 39:5121–5132
Haddad S, Willett RD (2001) Polymorphism in bis (4-dimethyl aminopyridinium) tetrachlorocuprate (II). Inorg Chem 40:2457–2460
Hancock RD, Motekaitis RJ, Mashishi J, Cukrowski I, Reibenspies JH, Martell AE (1996) The unusual protonation constants of cyclam. A potentiometric, crystallographic, and molecular mechanics study. J Chem Soc Perkin Trans 2:1925–1929
Hawkesworth G, Draser BS (1971) Intestinal bacteria and the hydrolysis of glycosidic bonds. J Med Microbiol 4(4):451–459
Helfand SL, Werkmeister J, Roder JC (1982) Chemiluminescence response of human natural killer cells. The relationship between target cell binding, chemiluminescence, and cytolysis. J Exp Med 156:492–505
Hua L, Kiyoushi HT, Ken M, Verne C, Richard TS (1990) The properties of beta-glucuronidase. Further evidence of its involvement in compartmentalization of beta-glucuronidase and sequence similarity with portions of the reactive site region of the serpin superfamily. J Biol Chem 265(25):14732–14735
Karlin KD, Tyelkar Z (eds) (1993) Bioinorganic chemistry of copper. Chapman and hall, New York
Khan I, Ali S, Hameed S, Rama NH, Hussain MT, Wadood A, Uddin R, Ul-Haq Z, Khan A, Ali S, Choudhary MI (2010) Synthesis, antioxidant activities and urease inhibition of some new 1,2,4-triazole and 1,3,4-thiadiazole derivatives. Eur J Med Chem 45:5200–5207
Kim DH, Jung EA, Sohng IS, Han JA, Kim TH, Han MJ (1998) Intestinal bacterial metabolism of flavonoids and its relation to some biological activities. Arch Pharm Res 21(1):17–23
Leung JW, Liu Y-l, Leung PSC et al (2001) Expression of bacterial β-glucuronidase in human bile: an in vitro study. Gastrointest Endosc 54(3):346–350
Liang X, Sadler PJ (2004) Cyclam complexes and their applications in medicine. Chem Soc Rev 33:246–266
Liang X, Parkinson JA, Weishaupl M, Gould RO, Paisey SJ, Park HS, Hunter TM, Blindauer CA, Parsons S, Sadler PJ (2002) Structure and dynamics of metallomacrocycles: recognition of zinc xylyl-bicyclam by an HIV coreceptor. J Am Chem Soc 124:9105–9112
Lien-Vien D, Colthup NB, Fateley WG, Grasselli JG (1991) The handbook of infrared and Raman characteristic frequencies of organic molecules, 1st edn. Academic Press, Boston, MA
Lincoln SF (1997) Mechanistic studies of some macrocyclic complexes. Coord Chem Rev 166:255–289
Lindoy LF (1998) The transition-metal ion chemistry of linked macrocyclic ligands. Adv Inorg Chem 45:75–125
Lukes I, Kotek J, Vojtisek P, Hermann P (2001) Complexes of tetraazacycles bearing methylphosphinic/phosphonic acid pendant arms with copper(II), zinc(II) and lanthanoids(III). A comparison with their acetic acid analogues. Coord Chem Rev 216–217:287–312
Martell AE, Hancock RD (1996) Metal complexes in aqueous solutions. Plenum Press, New York
Mathieu B, Rik G, Hugo C, Willy S, Cristiana S (2000) Nucleotide pyrophosphatases/phosphodiesterases on the move. Crit Rev Biochem Mol Biol 35(6):393–432
McBain AJ, Macfarlane GT (1998) Ecological and physiological studies on large intestinal bacteria in relation to production of hydrolytic and reductive enzymes involved in formation of genotoxic metabolites. J Med Microbiol 47(5):407–416
Melson GA (ed) (1979) Coordination chemistry of macrocyclic compounds. Plenum, New York
Mesaik MA, Rahat S, Khan KM, Zia-Ullah, Choudhary MI, Murad S, Ismail Z, Atta-ur-Rahman, Ahmad A (2004) Synthesis and immunomodulatory properties of selected oxazolone derivatives. Bioorg Med Chem 12(9):2049–2057
Meyer M, Dahaoui-Ginderey V, Lecomte C, Guilard R (1998) Conformation and coordination schemes of carboxylate and carbamoyl derivatives of the tetraazamacrocycles cycles and cyclam, and the relation to their protonation states. Coord Chem Rev 178–180:1313–1405
Moi MK, Meares CF, McCall MJ, Cole WC, DeNardo SJ (1985) Copper chelates as probes of biological systems: stable copper complexes with a macrocyclic bifunctional chelating agent. Anal Biochem 148:249–253
Mosmann T (1983) Rapid colorimetric assay for cellular growth and survival: application to proliferation and cytotoxicity assays. J Immunol Meth 65:55–63
Nakamoto K (1997) Infrared and Raman spectra of inorganic and coordination compounds. Part B, 5th edn. Wiley, New York
Nather C, Jess I (2004) Crystal structure and thermal reactivity of new copper(I) halide pyrimidine-containing coordination polymers. Eur J Inorg Chem 14:2868–2876
Orpen AG, Brammer L, Allen FH, Kennard O, Watson DG, Taylor R (1989) Organometallic compounds and co-ordination complexes of the d- and f-block metals. J Chem Soc Dalton Trans 12:1–83
Oxford Diffraction (2005) CrysAlis CCD and CrysAlis RED. Oxford Diffraction, Abingdon, Oxfordshire, England
Petricek V, Dusek M, Palatinus L (2006) Jana2006. The Crystallographic Computing System. Institute of Physics, Praha, Czech Republic
Rahbar S, Figarola JL (2003) Novel inhibitors of advanced glycation endproducts. Arch Biochem Biophys 419:63–79
Riaz N, Anis I, Aziz-ur-Rehman, Malik A, Ahmed Z, Muhammad P, Shujaat S, Atta-ur-Rahman (2003) Emodinol, β-glucuronidase, inhibiting triterpine from *Paeonia emodi*. Nat Pro Res 17(4): 247–251
Robin MB, Day P (1967) Mixed valence chemistry—a survey and classification. Adv Inorg Chem Radiochem 10:247–422
Rod TO, Midtvedt T (1977) Origin of intestinal β-glucuronidase in germfree, monocontaminated and conventional rats. Acta Pathol Microbiol Scand B 85(4):271–276
Sell S (1987) Immunomodulation. In: Immunology immunopathology and immunity. Elsevier Science. Publishing Co. Inc., New York, pp 655–683
Studer M, Riesen A, Kaden T (1989) Synthesis and structure of halocuprates of tetraprotonated 1,4,8,11-tetraazacyclotetradecane and its Cu^{2+} complex. Helv Chim Acta 72:1253–1258
Subramanian L, Hoffmann R (1992) Bonding in halocuprates. Inorg Chem 31:1021–1029
Wainwright KP (1997) Synthetic and structural aspects of the chemistry of saturated polyaza macrocyclic ligands. Coord Chem Rev 166:35–90
Wallace BD, Wallace BD, Wang H, Lane KT, Scott JE, Orans J, Koo JS, Venkatesh M, Jobin C, Yeh LA, Mani S, Redinbo MR (2011) Alleviating cancer drug toxicity by inhibiting a bacterial enzyme. Science 330:831–835
Wansi JD, Mesaik MA, Chiozem DD, Devkota KP, Kolar NG, Lallemand MC, Wandji J, Choudhary MI, Sewald N (2008) Oxidative burst inhibitory and cytotoxic indoloquinazoline and furoquinoline alkaloids from *Oricia suaveolens*. J Nat Prod 71(11):1942–1945
Yatsimirskii KB, Lampeka YD (1985) Physicochemitsry of metal complexes with macrocyclic ligands. Naukova Dumka, Kiev